J. Shanghai Jiaotong Univ. (Sci.), 2010, 15(2): 218-223
DOI: 10.1007/s12204-010-9716-z

Bleeding Detection from Wireless Capsule Endoscopy Images Using Improved Euler Distance in CIELab

*PAN Guo-bing** (潘国兵), *YAN Guo-zheng* (颜国正), *SONG Xin-shuai* (宋昕帅), *QIU Xiang-ling* (邱祥玲)
(School of Electronic Information and Electrical Engineering, Shanghai Jiaotong University, Shanghai 200240, China)

Abstract: Bleeding in the digestive tract is one of the most common gastrointestinal (GI) tract diseases, as well as the complication of some fatal diseases. Wireless capsule endoscopy (WCE), which is widely applied in the clinical field, allows physicians to noninvasively examine the entire GI tract. However, it is very laborious and time-consuming to detect the huge amount of WCE images, and limits its wider application. It is urgent and necessary to develop the automatic and intelligent computer aided bleeding detection technique. This paper improves the Euler distance with the covariance matrix of image to measure the colour similarity in CIELab colorimetric system, and proposes a novel method of bleeding detection in WCE images. The experiments demonstrate that the bleeding region in WCE images can be correctly recognized and marked out, and the sensitivity of this method is 92%, the specificity is 95%.
Key words: bleeding detection, wireless capsule endoscopy image, CIELab, covariance matrix
CLC number: TP 391, R 57 **Document code:** A

1 Introduction

Bleeding in the digestive tract is not only a common gastrointestinal (GI) trace disease, but also a well-recognized complication, which is a symptom of fatal diseases[1]. Most causes of bleeding are related to conditions that can be cured or controlled, yet to detect the bleeding is not easy. The best way to detect bleeding is directly imaging the GI tract, so the endoscopy is a direct and effective diagnostic technique comparing to indirect techniques such as barium angiography and computerized tomography[2]. In 2000, the first wireless capsule endoscopy (WCE) M2A® is released by the Israel Given Image Company, and the first clinical experiments are implemented in 2001[3-4]. The capsule endoscope developed by Shanghai Jiaotong University is 12 mm in diameter and 28 mm in length which is small enough to be easily swallowed by patients. After being swallowed, the capsule endoscope travels through the whole GI tract with the GI tract nature peristalsis. During the course it transmits 2 frames of images outside the patient's body every second, and the image data are received and stored in the receiving box which is tied to the patient's waist. The image data are downloaded into the work station and shown by the software application. The usage of WCE is convenient and painless and the whole GI tract is examined without a dead zone in the endoscopic diagnosis. The WCE is applied more and more in clinical examinations based on these assets[5-10].

During the 8-hour examination, the WCE generates at least $2 \times 3\,600 \times 8 = 57\,600$ images. It is very laborious and time-consuming to find the bleeding regions from the huge amount of WCE images. It takes more than 3 hours to detect these images even by a skilled expert. This is not only time-consuming but also leading false detection because of visual fatigue. Therefore, it is urgent and necessary to develop computer aided intelligent bleeding recognition algorithm to process the WCE images automatically. The Given Image Company provides a software tool to detect the bleeding called Suspected Blood Indicator (SBI). However it was reported to have lower sensitivity of 72% and specificity of 85%[11]. As a consequence it does not free physicians from reviewing the entire footage and should only be used as a fast screening tool. The Ref. [12] used adaptive color histogram model to detect bleeding. The algorithm firstly uses HSI (hue, saturation,

Received date: 2009-02-20
Foundation item: the National High Technology Research and Development Program (863) of China (No. 2006AA04Z368), the National Natural Science Foundation of China (No. 30570485)
∗**E-mail:** guobpan@gmail.com

intensity) color histogram to track a moving background and bleeding color distributions over time, secondly extracts color and texture features from suspicious WCE images, finally classifies them using support vector classification into bleeding , lesion and normal classes. The procedure is obviously too complex to be practical in clinical fields. Further, the paper doesn't give detailed test and the experiment just show the method is better than SBI. The Ref. [13] presented a method based on neural network to detect bleeding. But the authors did not present the neural network model and just give some experiments. Unfortunately, only 13 images were used as training set and 3 images were used to test the method, furthermore the experiments showed that the sensitivity of this methodology was lower than 80%. The Ref. [14] built a multi-layer perceptron (MLP) neural network with three layers to recognize bleeding regions. MLP is a modification of the standard linear perceptron, which has poor robustness and anti-interference ability, and is not suitable for the nonlinear classification. Although the detection rate of this MLP method reached 90%, the authors did not give the specificity of this method. There are other study works on this topic, but few satisfactory results are obtained.

In order to improve the bleeding detection rate, this paper improves Euler distance to measure the colour similarity in CIELab colorimetric system, and proposes a novel and efficient method of bleeding recognition based on the improved distance. This method of bleeding recognition is implemented and the experiments show that the sensitivity of this method is 92% and the specificity is 95%.

2 Improved Euler Distance in CIELab

2.1 CIELab Colorimetric System

The colorimetric system is an abstract mathematical representation of colour. For colour image recognition, selecting suitable colorimetric system is the first step, and then accordingly develops algorithms for this colorimetric system. CIEXYZ is a standard colorimetric system, and images in CIERGB can be transformed into CIEXYZ according to the following transformation equation[15].

$$\begin{bmatrix} X \\ Y \\ Z \end{bmatrix} = \begin{bmatrix} 2.768\,9 & 1.751\,7 & 1.130\,2 \\ 1.000\,0 & 4.590\,7 & 0.060\,1 \\ 0.000\,0 & 0.056\,5 & 5.594\,3 \end{bmatrix} \begin{bmatrix} R \\ G \\ B \end{bmatrix}. \quad (1)$$

CIERGB and CIEXYZ are trichromatic systems, in which R, G, B and X, Y, Z are the three reference colour stimuli. They are neither uniform colorimetric systems, that is the distance between two pixels differs greatly from the colour difference between them. CIELab colorimetric system based on CIEXYZ is a widely used uniform system, which is also called $L^*a^*b^*$ colour space. L^*, a^* and b^* are defined as follows.

$$L^* = \begin{cases} 116\left(\dfrac{Y}{Y_\mathrm{n}}\right)^{\frac{1}{3}} - 16, & \dfrac{Y}{Y_\mathrm{n}} > 0.008\,856 \\ 903.29\dfrac{Y}{Y_\mathrm{n}}, & \dfrac{Y}{Y_\mathrm{n}} \leqslant 0.008\,856 \end{cases}, \quad (2)$$

$$a^* = 500\left[f(X/X_\mathrm{n}) - f(Y/Y_\mathrm{n})\right], \quad (3)$$

$$b^* = 200\left[f(Y/Y_\mathrm{n}) - f(Z/Z_\mathrm{n})\right], \quad (4)$$

$$f(\alpha) = \begin{cases} \alpha^{1/3}, & \alpha > 0.008\,856 \\ 7.78\alpha + 13/116, & \alpha \leqslant 0.008\,856 \end{cases}, \quad (5)$$

where X_n, Y_n and Z_n are the tristimulus values of the reference white point, and the mostly used white point is D65[15].

2.2 Covariance Matrix of Image

Let vector $\boldsymbol{X}_i$ denote pixels in the image to be detected, where $i = 1, 2, \cdots, MN$, M and N are the width and length of the image. $\boldsymbol{X}_i = [x_{iL^*} \;\; x_{ia^*} \;\; x_{ib^*}]$, where x_{iL^*}, x_{ia^*} and x_{ib^*} are the three components of the pixels in $L^*a^*b^*$ colour space. The discrete probability distribution $\boldsymbol{P}(\boldsymbol{X}_i)$ is the $M \times N$ 3D vectors of the image. Assumed there are k bleeding pattern pixels in one image, let $\boldsymbol{X}_j$ denote the bleeding pattern pixels, where $j = 1, 2, \cdots, k$, the mathematical expectation of $\boldsymbol{X}_j$ can be calculated as

$$E[\boldsymbol{X}_j] = \frac{1}{k}\sum_{j=1}^{k} \begin{bmatrix} x_{jL^*} \\ x_{ja^*} \\ x_{jb^*} \end{bmatrix}. \quad (6)$$

The covariance matrix $\boldsymbol{\Sigma}$ of pattern vectors in the image can be defined as

$$\boldsymbol{\Sigma} = E[(\boldsymbol{X}_i - E[\boldsymbol{X}_j])(\boldsymbol{X}_i - E[\boldsymbol{X}_j])^\mathrm{T}] = \begin{bmatrix} C_{L^*L^*} & C_{L^*a^*} & C_{L^*b^*} \\ C_{a^*L^*} & C_{a^*a^*} & C_{a^*b^*} \\ C_{b^*L^*} & C_{b^*a^*} & C_{b^*b^*} \end{bmatrix}, \quad (7)$$

$$C_{mn} = E[(x_{im} - E[x_{im}])(x_{in} - E[x_{in}])], \quad m, n = L^*, a^*, b^*. \quad (8)$$

Because x_{iL^*}, x_{ia^*} and x_{ib^*} are independently random variables, the covariance between them are 0, namely when $m \neq n$, $C_{mn} = 0$, and then the covariance matrix can be simplified as

$$\boldsymbol{\Sigma} = \begin{bmatrix} C_{L^*L^*} & & \\ & C_{a^*a^*} & \\ & & C_{b^*b^*} \end{bmatrix}, \quad (9)$$

$$C_{mm} = E[(x_{im} - E[x_{jm}])^2] = \frac{1}{MN}\sum_{i}^{MN}[x_{im} - E[x_{jm}]]^2, \quad (10)$$
$$m = L^*, a^*, b^*.$$

$\boldsymbol{\Sigma}$ shown in Eq. (9) is the covariance matrix of the image to be recognized, and C_{mm} is the variance of $\boldsymbol{X}_i$.

2.3 Improved Euler Distance

Consider $E[\boldsymbol{X}_j]$ as the cluster center of the bleeding pattern, to detect the pattern of pixels is to measure the similarity between the vectors of $\boldsymbol{X}_i$ and $E[\boldsymbol{X}_j]$. In $L^*a^*b^*$ colour space, the colour difference between two colours is represented by Δd^*_{ab}, which is also known as Euler distance and is defined as[15]

$$\Delta d^*_{ab} = [\Delta L^{*2} + \Delta a^{*2} + \Delta b^{*2}]^{1/2} = [(\boldsymbol{X}_i - E[\boldsymbol{X}_j])(\boldsymbol{X}_i - E[\boldsymbol{X}_j])^{\mathrm{T}}]^{1/2}. \quad (11)$$

By adding the covariance matrix $\boldsymbol{\Sigma}$ into the Euler distance, a new distance can be gotten to represent the colour difference between $\boldsymbol{X}_i$ and $E[\boldsymbol{X}_j]$:

$$\Delta d^*_{ab} = [(\boldsymbol{X}_i - E[\boldsymbol{X}_j])\boldsymbol{\Sigma}(\boldsymbol{X}_i - E[\boldsymbol{X}_j])^{\mathrm{T}}]^{1/2} = \left\{(\boldsymbol{X}_i - E[\boldsymbol{X}_j])\begin{bmatrix} C_{L^*L^*} & & \\ & C_{a^*a^*} & \\ & & C_{b^*b^*} \end{bmatrix} \times (\boldsymbol{X}_i - E[\boldsymbol{X}_j])^{\mathrm{T}}\right\}^{1/2} = (C_{L^*L^*}\Delta L^{*2} + C_{a^*a^*}\Delta a^{*2} + C_{b^*b^*}\Delta b^{*2})^{1/2}. \quad (12)$$

Δd^*_{ab} in Eq. (12) is a new definition of distance which can be used to measure the colour similarity. Compared to Euler distance, the improved distance makes the difference between bleeding pattern and non-bleeding patter wider. Figure 1 is a typical bleeding WCE image, and the improved Euler distance map accordingly is shown in Fig. 2. The distance map clearly shows that the distances from bleeding pixels to bleeding cluster center $E[\boldsymbol{X}_j]$ are significantly lower than others and the difference between the two patterns are clear.

3 Bleeding Detection

3.1 Feature Extraction

The typical bleeding WCE image shown in Fig. 1 clearly shows that the most salient feature of the bleeding region is the colour difference. Red as the whole image is, the saturation of the bleeding region looks higher comparing to the non-bleeding region, which is shown on the top right corner. Comparing pixel $\boldsymbol{X}_i$ with the bleeding pattern cluster center $E[\boldsymbol{X}_j]$ to measure the colour similarity, if the colour similarity is low, the two pixels are not similar, therefore the pixel is recognized as non-bleeding pixel; otherwise the two pixels are similar, the pixel is recognized as bleeding pattern. The distance map in Fig. 2 shows clearly that more similar $\boldsymbol{X}_i$ and $E[\boldsymbol{X}_j]$ are, smaller the distance between them is; on the contrary, less similar they are, lager the distance is.

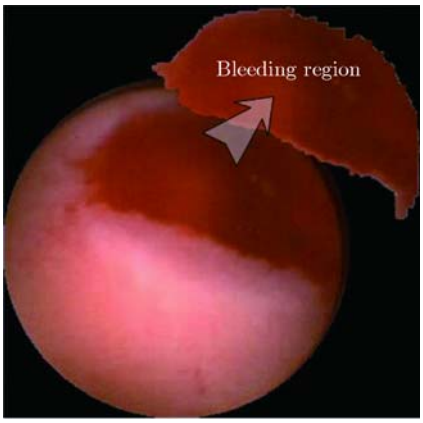

Fig. 1 Typical bleeding image

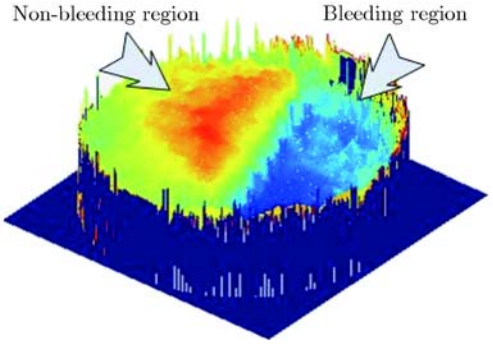

Fig. 2 Distance map

The calculation of Eq. (6) indicates the bleeding pattern cluster center of the bleeding image in Fig. 1 is $E[\boldsymbol{X}_j] = [108\ 72\ 79]$. So the feature of bleeding pixels is that they are similar to the bleeding pattern cluster center $E[\boldsymbol{X}_j]$, namely the distances to [108 72 79] are short.

3.2 Bleeding Detection Implementation

Comparing all bleeding pixels $\boldsymbol{X}_j$ in Fig. 1 with [108 72 79], $d_{\max} = 3\,500$ is the maximal distance. Let

$d_{\max} = 3\,500$ be the threshold value of the classifying function, therefore the classifying function $d(\boldsymbol{X}_i)$ can be represented as

$$d(\boldsymbol{X}_i) = d_{\langle \boldsymbol{X}_i, E[\boldsymbol{X}_j]\rangle} - d_{\max} = d_{\langle \boldsymbol{X}_i, E[\boldsymbol{X}_j]\rangle} - 3\,500, \tag{13}$$

where $d_{\langle \boldsymbol{X}_i, E[\boldsymbol{X}_j]\rangle}$ denotes the distance from the pixel $\boldsymbol{X}_i$ to the bleeding pattern cluster center $E[\boldsymbol{X}_j]$. If $d(\boldsymbol{X}_i)$ is negative, the distance $d_{\langle \boldsymbol{X}_i, E[\boldsymbol{X}_j]\rangle}$ is small enough to recognize the pixel $\boldsymbol{X}_i$ as the bleeding pattern; on the contrary, if $d(\boldsymbol{X}_i)$ is nonnegative, the pixel $\boldsymbol{X}_i$ is recognized as non-bleeding pattern. Consider $\mathrm{d\_out}(\boldsymbol{X}_i)$ being the pattern classifier, and $\mathrm{d\_out}(\boldsymbol{X}_i) = B$ is defined as bleeding pattern and $\mathrm{d\_out}(\boldsymbol{X}_i) = N$ as non-bleeding pattern, therefore, the pattern classifier based on the distance can be formulized as

$$\mathrm{d\_out}(\boldsymbol{X}_i) = \begin{cases} B, & d(\boldsymbol{X}_i) > 0 \\ N, & d(\boldsymbol{X}_i) \leqslant 0 \end{cases}. \tag{14}$$

Based on the classifier in Eq. (14), the WCE image is scanned pixel by pixel, measuring the similarity, and put the measurement results into the classifier $\mathrm{d\_out}(\boldsymbol{X}_i)$ to judge. Go on measuring and judging pixel by pixel until the first bleeding pixel in the WCE image is gotten. Take this bleeding pixel as the first seed, and take the output of the classifier $\mathrm{d\_out}(\boldsymbol{X}_i)$ as the growing law to go on the seeded-region-growing algorithm. If the output of the classifier is B or N, the pixel is accordingly recognized as bleeding pattern or non-bleeding pattern. After a new bleeding pattern pixel is gotten, it is taken as a new seed and the seeded-region-growing steps continue until the whole WCE image is finished. Finally calculate the area of every bleeding region, if the area is too small, this bleeding region is not really bleeding pattern and will be filtered out, because it's impossible for bleeding pixels emerges insularly or only few number. These steps are illustrated as Fig. 3.

After these steps, the WCE images will be included into the bleeding images if there are bleeding regions, otherwise it will be included into the non-bleeding images.

According to the bleeding detection algorithm and the implementation steps, the bleeding detection application software is programmed, and the WCE images shown in Fig. 4 are detected. The images in Fig. 4 are the confirmed bleeding WCE images, and the detection results are shown in Fig. 5. In the results, red and green regions are the bleeding region and non-bleeding region respectively. After being filtered out, the small area bleeding regions are marked as the green non-bleeding regions. The results show that the bleeding and non-bleeding regions are clearly and correctly marked out.

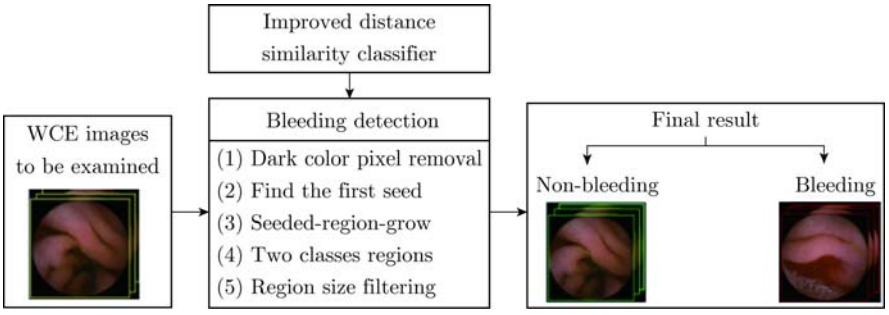

Fig. 3 Frameworks of the bleeding detection algorithm

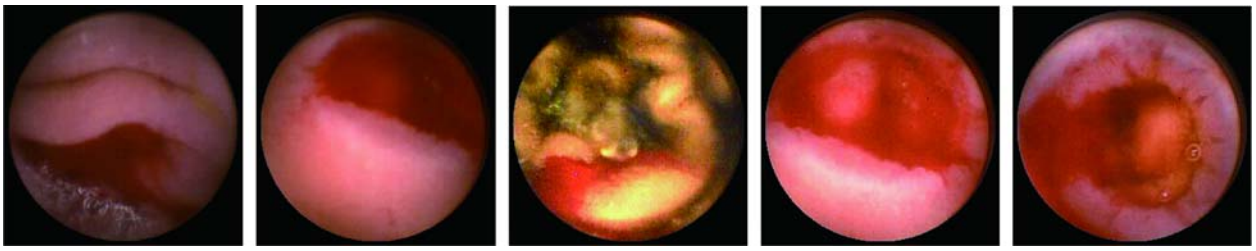

Fig. 4 Images to be detected

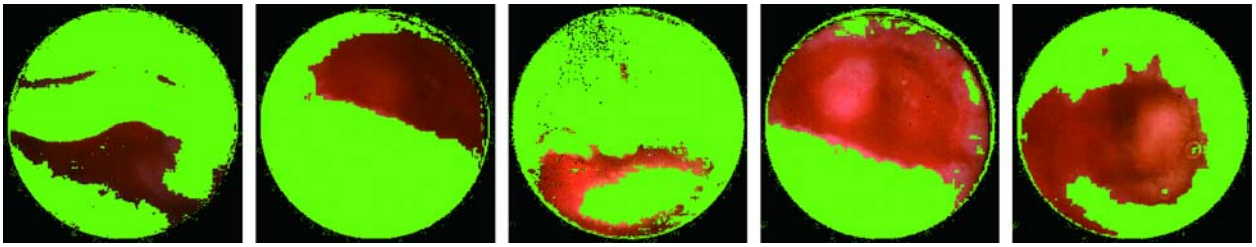

Fig. 5 Detection result

4 Experiments and Analysis

Medical diagnostic applications are often perceived by physicians as providing absolute answers. The absolute answer of the bleeding detection is bleeding image or non-bleeding image. As a consequence, the bleeding images can be possibly recognized as non-bleeding images which are called false non-bleeding (Fnb) recognition, and the non-bleeding images can be possibly recognized as bleeding images which are called false bleeding (Fb) recognition. Others cases are true recognitions, and the true bleeding recognition is presented by Tb, and the true non-bleeding recognition is presented by Tnb. To assess the capability of the bleeding detection algorithm, namely the performance of the classifier, sensitivity $\eta_{\rm se}$ and specificity $\eta_{\rm sp}$ are adequate which are estimated as[16]

$$\eta_{\rm se} = \frac{\sum \mathrm{Tb}}{\sum \mathrm{Tb} + \sum \mathrm{Fnb}}, \tag{15}$$

$$\eta_{\rm sp} = \frac{\sum \mathrm{Tnb}}{\sum \mathrm{Tnb} + \sum \mathrm{Fb}}. \tag{16}$$

For the assessing of the performance of the bleeding detection method, we obtain 10 full video clips consisting of 960 WCE images which are available on the endoscopy organization website. There are 546 bleeding images and 414 non-bleeding images detected manually. Run the bleeding detection software on these full length video clips and the detection result is shown in the Table 1, $\eta_{\rm se} = 91.94\%$, $\eta_{\rm sp} = 94.92\%$.

Table 1 Result of the detection

	Bleeding/frame	No-bleeding/frame
Detected as bleeding	502	21
Detected as no-bleeding	44	393

The most image misclassifications mostly occur when the old hemorrhage is present in the WCE images and the bleeding regions are too dark. Compared with existing algorithms, this algorithm is more suitable for video WCE images detection because of the clear concept, low computation complexity and practicability. Furthermore, this algorithm can realize the real time detection during the WCE examination course.

5 Conclusion

It is urgent and necessary to develop the automatic and intelligent computer aided bleeding detection in WCE diagnosis. The most salient feature of the bleeding region in WCE images is the colour difference, the bleeding pattern pixels are similar to the cluster center $E[\boldsymbol{X}_j]$ while the non-bleeding pattern pixels have low similarity to it. After studying the colour similarity measurement deeply, this paper improves the Euler distance to suit the image recognition in CIELab colorimetric system, and builds a pattern classifier based on the improved Euler distance to recognize the bleeding WCE images. This novel method of bleeding detection from WCE images is implemented in CIELab colorimetric system, and the experiments demonstrate that the bleeding region in WCE images can be correctly detected and marked out, and the sensitivity of the algorithm is 92%, the specificity is 95%.

References

[1] National Digestive Diseases Information Clearinghouse. Bleeding in the digestive tract [M]. Bethesda, Maryland: National Institutes of Health, 2007: 1-6.

[2] Eliakim R, Suissa A, Yassin K, *et al.* Wireless capsule video endoscopy compared to barium follow-through and computerised tomography in patients with suspected Crohn's disease–final report [J]. *Digestive and Liver Disease*, 2004, **36**(8): 519-522.

[3] Iddan G, Meron G, Glukhovsky A, *et al.* Wireless capsule endoscopy [J]. *Nature*, 2000, **405**(6785): 417.

[4] Swain P, Iddan G J, Meron G, *et al.* Wireless capsule endoscopy of the small bowel: development, testing, and first human trials [C]// *Biomonitoring and Endoscopy Technologies.* Amsterdam, Netherlands: SPIE, 2001: 19-23.

[5] Delvaux M, Gay G. Capsule endoscopy in 2005: Facts and perspectives [J]. *Best Practice & Research in Clinical Gastroenterology*, 2006, **20**(1): 23-39.

[6] Pennazio M. Capsule endoscopy: Where are we after 6 years of clinical use? [J]. *Digestive and Liver Disease*, 2006, **38**(12): 867-878.

[7] Sturniolo G C, Leo V D, Vettorato M G, *et al.* Small bowel exploration by wireless capsule endoscopy: Results from 314 procedures [J]. *American Journal of Medicine*, 2006, **119**(4): 341-347.

[8] Abdullah B, Ruzyla T. Wireless capsule endoscopy: A pediatric experience [J]. *American Journal of Gastroenterology*, 2008, **103**: S53.

[9] Golding M, Doman D, Goldberg H. Use of wireless capsule endoscopy for evaluation of sustained gastric presence of a polymer medication delivery system [J]. *American Journal of Gastroenterology*, 2008, **103**: S41.

[10] Muhammad A, Khara H, BajaJ P, *et al.* A single-center experience of 831 patients with wireless capsule endoscopy [J]. *American Journal of Gastroenterology*, 2008, **103**: S510.

[11] Buscaglia J M, Giday S A, Kantsevoy S V, *et al.* Performance characteristics of the suspected blood indicator feature in capsule endoscopy according to indication for study [J]. *Clinical Gastroenterology and Hepatology*, 2008, **6**(3): 298-301.

[12] Mackiewicz M, Fisher M, Jamieson C. Bleeding detection in wireless capsule endoscopy using adaptive colour histogram model and support vector classification [C]// *Medical Imaging 2008 Conference.* San Diego, CA: SPIE-Int Soc Optical Engineering, 2008: R1-R12.

[13] Bourbakis N, Makrogiannis S, Kavraki D, *et al.* A neural network-based detection of bleeding in sequences of WCE images [C]// *5th IEEE Symposium on Bioinformatics and Bioengineering.* Minneapolis, MN: IEEE Computer Soc, 2005: 324-327.

[14] Li B P, Meng Q H. Computer aided detection of bleeding in capsule endoscopy images [C]// *2008 Canadian Conference on Electrical and Computer Engineering.* Niagara Falls, Canada: IEEE, 2008: 1875-1878.

[15] Takagi M, Shimoda H. Handbook of image analysis [M]. Beijing: Science Press, 2007: 428-440 (in Chinese).

[16] Altman D G, Bland J M. Diagnostic tests. 1. Sensitivity and specificity [J]. *BMJ*, 1994, **308**(6943): 1552.